Channel Modelling of Human Tissues at Terahertz Band

Ke Yang, Yang Hao, Akram Alomainy
School of Electronic Engineering and Computer Science
Queen Mary University of London
Mile End Road, London E1 4NS
Email: {k.yang, y.hao, a.alomainy }@qmul.ac.uk

Qammer H. Abbasi, Khalid Qaraqe
Electrical and Computer Engineering
Texas A & M University at Qatar
Doha, Qatar
Email: {qammer.abbasi, khalid.qaraqe}@qatar.tamu.edu

***Abstract*—In this paper, the channel model is proposed to compute the path loss, delay and noise at THz band of interest (0.5 THz $\sim$ 1.5 THz). The results shows that THz band channel is strongly dependent on both the type of the medium and the distance while the concentration of water have a lot of influence because it not only causes attenuation to the THz wave but also introduces non-white noise. Therefore, the proposed model paves the way to the further studies considering more body structures and tissue properties.**

I. Introduction

It has been found out that graphene-based plasmonic nano-antennas are expected to work at THz band [1], [2], [3]; thus, THz band is considered as a promising candidate for nano-communication. At the same time, a substantial amount of work has been performed on the channel characterization and modeling for body-centric wireless communications at microwave frequencies and mm-wave band [4]. Statistical on-body path loss models for different links and body scenarios have been developed by analyzing the measurement data from on-body propagation with two patch antennas working at 2.45 GHz in an anechoic and lab environment [5]. The path loss model of radio propagation in human tissues was presented in [6] and subsequently compared to experimental results for muscle, validating the reliability of the numerical simulation at 2.45 GHz. A numerical modeling method using parallel FDTD was applied to study the radio propagation and system performance of the wireless body area network at UWB band [7], proving that both channel performance and system performance are subject-specific. The path loss model for mm-wave was studied by comparing the numerical results from Remcom XGTD and measured data in [8], which indicated the path loss model for on-body communication at 94 GHz was closely related to the body shape and garments. At the same time, several papers on THz indoor communications have been published [9], [10]. In addition, the optical parameters of human tissues up to 2.5 THz have been empirically characterized in [11], [12] following the discussion of the possibility of applying EM waves in nano-networks [13]. The channel model for THz wave propagating in the air with different concentration of the water vapor was presented in [14] and the corresponding channel capacity was also studied. Based on the characteristics of the channel, a new physical- layer aware medium access control (MAC) protocol, Time Spread On-Off Keying (TS-OOK), was proposed [15]. Meanwhile, the applications of THz technology in imaging and medical field [16], [17] has also achieved great development and the biological effects of THz radiation are reviewed in [18] showing minimum effect on the human body and no strong evidence of hazardous side effects. However, most work presented in the open literature does not explicitly investigate the EM channel modeling at THz for the body-centric nano-networks, which would be the main contribution in this paper.

II. Path Loss

A modified Friis equation has been proposed by Jornet et al. in [14] to calculate the path loss of the THz channel in water vapor, which can be divided into two parts: the spread path loss PL_{spr} and the absorption path loss PL_{abs}. Similarly, the path loss in human tissues can also be divided into two parts:

$$PL_{total}[dB] = PL_{spr}(f,d)[dB] + PL_{abs}(f,d)[dB] \quad (1)$$

where, f stands for the frequency while d is the path length.

The spread path loss is introduced by the expansion of the wave in the medium, which is defined as:

$$PL_{spr}(f,d) = (\frac{4\pi d}{\lambda_g})^2 \quad (2)$$

where $\lambda_g = \lambda_o/n_r$ stands for the wavelength in medium with λ_o as the free-space wavelength and n_r as the real part of the infractive index, and d is the travelling distance of the wave. In this study, the electromagnetic power is considered to spread spherically with distance.

The absorption path loss accounts for the attenuation caused by the molecular absorption of the medium, where part of the energy of the propagating wave is converted into internal kinetic energy of the excited molecules in the medium. The absorption loss can be obtained from the transmittance of the medium $\tau(f,d)$:

$$PL_{abs} = \frac{1}{\tau(f,d)} = e^{\alpha(f)d} \quad (3)$$

The dependency of the channel path loss for blood, skin and fat on the distance and frequency is shown in Fig. 1. It is demonstrated that there are some fluctuations in each individual figure due to the fact that absorption path loss is related to the extinction coefficient, κ, which is not an analytical function along the required frequency band, in addition to the expected increase in path loss values with larger distances and higher frequency components. For different tissues, the path loss varies: with blood experiencing the highest losses, followed by the skin due to the water concentration, which contributes a significant absorption path loss. At the level of the millimeters, the path loss of the blood is around 120 dB, while the skin is around 90 dB and the fat is around 70 dB. Compared with the channel attenuation of the molecular communication [19], the future of the EM paradigms is promising because at 1 kHz (here, the frequency is the operation frequency of the RC circuit which depicted the emission and absorption process of the diffusion-based particle communication) and at a distance of 0.05 mm the molecular channel attenuation is above 140 dB which is substantially higher than the case for blood at the distance of $1mm$ applying THz EM communication mechanism. In [20], the capacity was also compared between the two paradigms, showing that that the EM communication keeps extremely high data rate until the distance is shorter than $10mm$ while the molecular communication scheme provides much lower capabilities.

III. Delay

As the name indicates, the propagation delay is the length of time it takes for waves travelling from the origin:

$$D = \frac{d}{\nu} \tag{4}$$

where, d is the path distance while $\nu = c/n_r$ is the wave speed in the medium.

The delay of blood, skin and fat are shown in Fig. 3. From the figures, it can be easily seen that the effect of the frequency on the delay can be ignored since the refractive index is considered as the same over this band here; but in fact the refractive index is not analytical over the band of interest. At the same time, the delay increase with the increase of the distance but is always at the level of pico-second which shows another advantage of EM communication over the molecular one. By comparing all three figures, we can see that for different tissue type, the delay is different: waves in fat took the shortest time while the wave in blood will travel for the longest time.

IV. Noise

The molecules along the path not only introduce the attenuation of the wave but also introduce the noise because their internal vibration, provoked by the incident wave, would turn into the emission of EM radiation at the same frequency [21], which can be measured by the parameter of the emissivity of the channel, ξ :

$$\xi(f, d) = 1 - \tau(f, d) \tag{5}$$

Where, $\tau(f, d) = e^{-\alpha(f)d}$ is the transmissivity of the medium, f is the frequency of the EM wave, d stands for the path length.

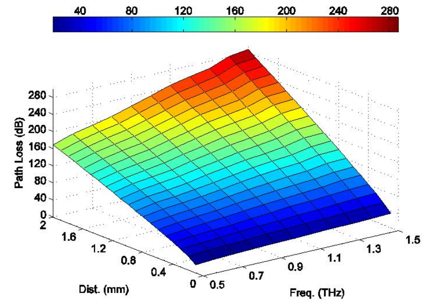

(a) Blood

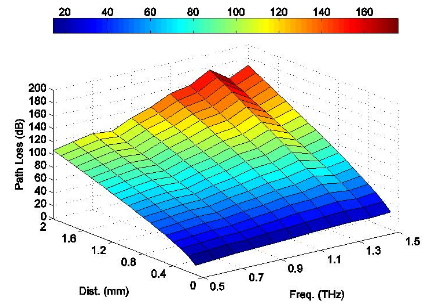

(b) Skin

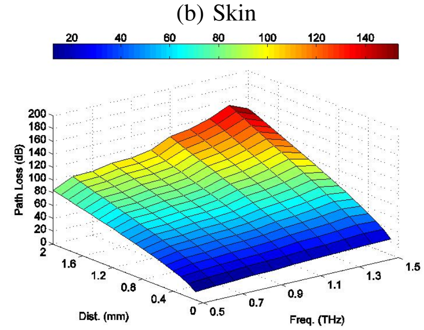

(c) Fat

Fig. 1: Total path loss as a function of the distance and frequency for different human tissues

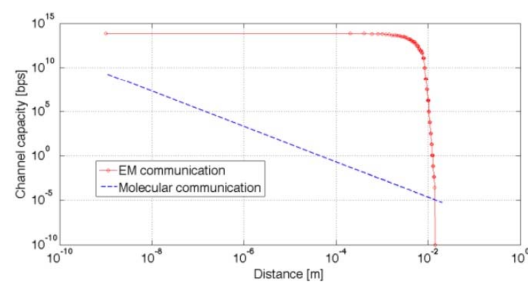

Fig. 2: Channel capacity comparison between EM and molecular communication [20]

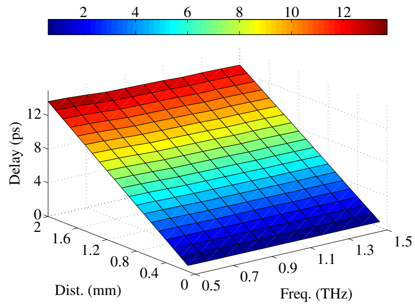

(a) Blood

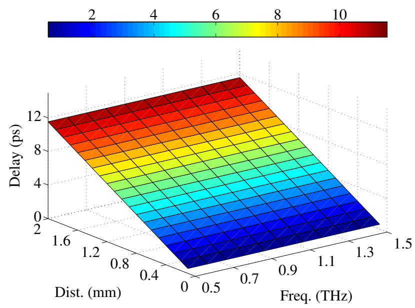

(b) Skin

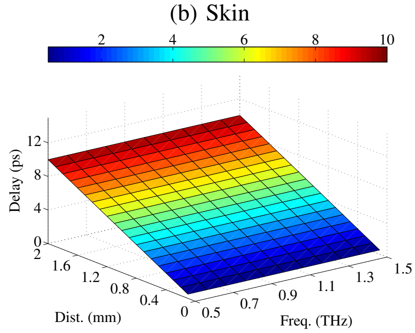

(c) Fat

Fig. 3: Delay as a function of the distance and frequency for different human tissues

Thus, the equivalent noise temperature due to molecular absorption can be obtained:

$$T_{mol}(f,d) = T_0 \xi(f,d) \tag{6}$$

where T_0 is the reference temperature, f is the frequency of the EM wave, d stands for the path length, ξ refers to the emissivity of the channel given by Eq. 5. It should be noted that this kind of noise only appears around the frequencies in which the molecular absorption is quite high.

The total noise temperature of the system T_{noise} is composed of the system electronic noise temperature, T_{sys}, and the total antenna noise temperature, T_{ant}, which includes not only the molecular absorption noise temperature, T_{mol}, but also other contributions from several sources, T_{other}, such as the noise created by surrounding nano-devices or the same device.

$$T_{noise} = T_{sys} + T_{ant} = T_{sys} + T_{mol} + T_{other} \tag{7}$$

For a given bandwidth, B, the total system noise power at the receiver can be calculated as follows:

$$P_n(f,d) = \int N(f,d)df = k_B \int T_{noise}(f,d)df \tag{8}$$

Where, N stands for the noise power spectral density; k_B is the Boltzmann constant; T_{noise} is the equivalent noise temperature.

Because the electronic noise temperature of the system is assumed to be low due to the electron transport properties of graphene [22], the main factor affecting the channel performance will be the molecular absorption noise temperature, which indicates $T_{noise} \approx T_{mol}$.

The molecular absorption noise temperature is shown in Fig. 4. It can be seen that the noise temperature increases with the rise of the frequency and distance, which will lead to the rise of the noise power. At the level of millimeters, the molecular noise temperature reaches 310 K, the normal human temperature.

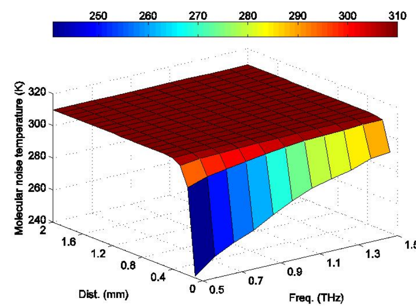

(a) Blood

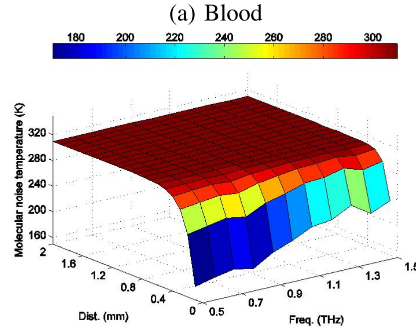

(b) Skin

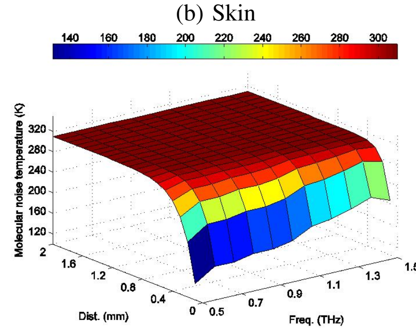

(c) Fat

Fig. 4: Noise temperature as a function of the distance and frequency for different human tissues

V. Conclusion

The channel performance on path loss, delay and noise were studied in this paper, showing the great potential of the application of THz wave for nano EM communication. The results showed that the channel performance not only related to the distance and frequency, but also depended on the tissue type, mainly the water concentration of the tissue.

Acknowledgment

Many thanks to the CSC (China Scholarship Council) for supporting the first author's research studies in Queen Mary University of London (QMUL), UK. This publication was made possible by NPRP grant # 7-125-2-061 from the Qatar National Research Fund (a member of Qatar Foundation). The statements made herein are solely the responsibility of the authors.

References

[1] Serge Luryi, Jimmy Xu, and Alexander Zaslavsky. *Future Trends in Microelectronics: Frontiers and Innovations*. John Wiley & Sons, 2013.

[2] M Dragoman, AA Muller, D Dragoman, F Coccetti, and R Plana. Terahertz antenna based on graphene. *Journal of Applied Physics*, 107(10):104313, 2010.

[3] Ignacio Llatser, Christian Kremers, Albert Cabellos-Aparicio, Josep Miquel Jornet, Eduard Alarcón, and Dmitry N Chigrin. Graphene-based nano-patch antenna for terahertz radiation. *Photonics and Nanostructures-Fundamentals and Applications*, 10(4):353–358, 2012.

[4] Peter S. Hall and Yang Hao. *Antennas and Propagation for Body-Centric Wireless Communication*. Artech House, 2012.

[5] Akram Alomainy, Yang Hao, Abdus Owadally, Clive G Parini, Yuri Nechayev, Costas C Constantinou, and Peter S Hall. Statistical analysis and performance evaluation for on-body radio propagation with microstrip patch antennas. *Antennas and Propagation, IEEE Transactions on*, 55(1):245–248, 2007.

[6] Divya Kurup, Wout Joseph, Günter Vermeeren, and Luc Martens. In-body path loss model for homogeneous human tissues. *Electromagnetic Compatibility, IEEE Transactions on*, 54(3):556–564, 2012.

[7] Qammer Hussain Abbasi, Andrea Sani, Akram Alomainy, and Yang Hao. Numerical characterization and modeling of subject-specific ultrawideband body-centric radio channels and systems for healthcare applications. *Information Technology in Biomedicine, IEEE Transactions on*, 16(2):221–227, 2012.

[8] Alessio Brizzi, Alessandro Pellegrini, Lianhong Zhang, and Yang Hao. Statistical path-loss model for on-body communications at 94 ghz. *Antennas and Propagation, IEEE Transactions on*, 61(11):5744–5753, 2013.

[9] Yonghoon Choi, Ji-Woong Choi, and John M Cioffi. A geometric-statistic channel model for thz indoor communications. *Journal of Infrared, Millimeter, and Terahertz Waves*, 34(7-8):456–467, 2013.

[10] Radoslaw Piesiewicz, Martin Jacob, Martin Koch, Joerg Schoebel, and Thomas Kürner. Performance analysis of future multigigabit wireless communication systems at thz frequencies with highly directive antennas in realistic indoor environments. *Selected Topics in Quantum Electronics, IEEE Journal of*, 14(2):421–430, 2008.

[11] AJ Fitzgerald, E Berry, NN Zinov'ev, S Homer-Vanniasinkam, RE Miles, JM Chamberlain, and MA Smith. Catalogue of human tissue optical properties at terahertz frequencies. *Journal of Biological Physics*, 29(2-3):123–128, 2003.

[12] Elizabeth Berry, Anthony J Fitzgerald, Nickolay N Zinov'ev, Gillian C Walker, Shervanthi Homer-Vanniasinkam, Caroline D Sudworth, Robert E Miles, J Martyn Chamberlain, and Michael A Smith. Optical properties of tissue measured using terahertz-pulsed imaging. In *Medical Imaging 2003*, pages 459–470. International Society for Optics and Photonics, 2003.

[13] Ian F Akyildiz and Josep Miquel Jornet. Electromagnetic wireless nanosensor networks. *Nano Communication Networks*, 1(1):3–19, 2010.

[14] Josep Miquel Jornet and Ian F Akyildiz. Channel modeling and capacity analysis for electromagnetic wireless nanonetworks in the terahertz band. *Wireless Communications, IEEE Transactions on*, 10(10):3211–3221, 2011.

[15] Josep Miquel Jornet, Joan Capdevila Pujol, and Josep Solé Pareta. Phlame: A physical layer aware mac protocol for electromagnetic nanonetworks in the terahertz band. *Nano Communication Networks*, 3(1):74–81, 2012.

[16] Cecil S Joseph, Anna N Yaroslavsky, Victor A Neel, Thomas M Goyette, and Robert H Giles. Continuous wave terahertz transmission imaging of nonmelanoma skin cancers. *Lasers in Surgery and Medicine*, 43(6):457–462, 2011.

[17] Euna Jung, Hongkyu Park, Kiwon Moon, Meehyun Lim, Youngwoong Do, Haewook Han, Hyuck Jae Choi, Byung-Hyun Min, Sangin Kim, Ikmo Park, et al. Thz time-domain spectroscopic imaging of human articular cartilage. *Journal of Infrared, Millimeter, and Terahertz Waves*, 33(6):593–598, 2012.

[18] Gerald J Wilmink and Jessica E Grundt. Invited review article: current state of research on biological effects of terahertz radiation. *Journal of Infrared, Millimeter, and Terahertz Waves*, 32(10):1074–1122, 2011.

[19] Massimiliano Pierobon and Ian F Akyildiz. A physical end-to-end model for molecular communication in nanonetworks. *Selected Areas in Communications, IEEE Journal on*, 28(4):602–611, 2010.

[20] S. Bush, J. Paluh, G. Piro, V. Rao, V. Prasad, and A. Eckford. Defining communication at the bottom. *Molecular, Biological and Multi-Scale Communications, IEEE Transactions on*, PP(99):1–1, 2015.

[21] Frank Box. Utilization of atmospheric transmission losses for interference-resistant communications. *Communications, IEEE Transactions on*, 34(10):1009–1015, 1986.

[22] Atindra Nath Pal and Arindam Ghosh. Ultralow noise field-effect transistor from multilayer graphene. *Applied Physics Letters*, 95(8):082105, 2009.